

Correlation of ex vivo and in vivo confocal microscopy imaging of Acanthamoeba

Item Type	Journal article
Authors	Al-Antary, Noor Tawfiq Mohamad;Heaselgrave, Wayne;Hau, Scott
Citation	Alantary, N., Heaselgrave, W. and Hau, S. (2022) Correlation of ex vivo and in vivo confocal microscopy imaging of Acanthamoeba. British Journal of Ophthalmology Published Online First: 24 June 2022. doi: 10.1136/bjophthalmol-2022-321402
DOI	10.1136/bjophthalmol-2022-321402
Publisher	BMJ Publishing Group
Journal	British Journal of Ophthalmology
Download date	2026-05-17 02:52:39
License	https://creativecommons.org/licenses/by-nc/4.0/
Link to Item	http://hdl.handle.net/2436/624831

1
2
3
4
5
6
7
8
9
10
11
12
13
14
15
16
17
18
19
20
21
22
23
24
25
26
27
28
29
30
31
32
33
34
35
36
37
38
39
40
41
42
43
44
45
46
47
48
49
50
51
52
53
54
55
56
57
58
59
60

**Correlation of *ex vivo* and *in vivo* confocal microscopy imaging of
*Acanthamoeba***

Noor Alantary,^{1,4} Wayne Heaselgrave,^{1*} Scott Hau^{2,3}

¹Dept of Biomedical Science & Physiology, University of Wolverhampton, UK

²Department of External Disease, NIHR Moorfields Clinical Research Facility,
Moorfields Eye Hospital, UK

³UCL Institute of Ophthalmology, London, United Kingdom

⁴Aston Medical School, Birmingham, United Kingdom

Running title: The visualisation of *Acanthamoeba* spp. using confocal microscopy.

Keywords: *Acanthamoeba*, Keratitis, and Confocal microscopy

***Corresponding author. Mailing address:**

Dept of Biomedical Science & Physiology, University of Wolverhampton

MA Building, City Campus South, Wulfruna Street, Wolverhampton, WV1 1LY

UK

Tel: +44 (0)1902 32 2709 Email: w.heaselgrave@wlv.ac.uk

Synopsis/Precis (35 words):

Ex vivo confocal microscopy imaging of porcine corneas inoculated with the various life cycle stages of *Acanthamoeba* can be used as a reference to identify similar structures seen on *in vivo* imaging in *Acanthamoeba* keratitis.

Confidential: For Review Only

Abstract:

Background/Aims: The aim of this study was to correlate the various forms of *Acanthamoeba* on *ex vivo* confocal microscopy (EVCM) with *in vivo* confocal microscopy (IVCM) and findings from cultured positive cases of *Acanthamoeba keratitis*.

Methods: *Acanthamoeba* live, dead, and empty cysts, and live trophozoites were prepared *in vitro* and inoculated into porcine cornea using a sterile 26-gauge needle and examined *ex vivo* using the Heidelberg Retina Tomograph II/Rostock Corneal Module. IVCM images from 12 cultured positive *Acanthamoeba* cases, obtained using the same instrument, were compared with EVCM findings. Phase contrast images were also obtained to compare with both EVCM and IVCM findings. The change in cyst morphology with depth was evaluated by imaging the same cysts over a defined cornea depth measurement.

Results: EVCM morphologies for live cysts included 4 main types - hyper-reflective central dot with hyper-reflective outer ring, hyper-reflective central dot with hypo-reflective outer region, stellate shaped hyper-reflective centre with hypo-reflective outer region, and hyper-reflective round/polygonal shaped cyst; one main type for dead cysts - hyper-reflective central dot with hypo-reflective outer region; two main types for empty cysts - hyper-reflective central dot with hyper-reflective outer ring/hypo-reflective outer region; and one main type for trophozoites - large coarse speckled area of heterogeneous hyper-reflective material. Matching IVCM images show good correlation with EVCM. Cyst morphology altered when imaged at different depths.

1
2
3 **Conclusion:** EVCM demonstrated the various forms of *Acanthamoeba* cyst and
4 trophozoites can be used as a reference to identify similar structures on IVCM.
5
6
7
8
9
10

11
12
13
14
15
16
17 **What is already known on this topic** – *Acanthamoeba* keratitis is a sight-threatening
18 disease and *in vivo* confocal microscopy has been shown to be a useful tool in
19 diagnosing the infection with both high sensitivity and specificity but this is dependent
20 on observer experience.
21
22
23
24
25
26
27
28
29

30 **What this study adds** – The limitation with current *in vivo* confocal microscopy
31 technology is the difficulty in distinguishing host cellular structures from
32 *Acanthamoeba* cysts and trophozoites. *Ex vivo* confocal microscopy findings of the
33 various life cycle stages of *Acanthamoeba* identified in this study can be used as a
34 reference to aid the identification of the various trophozoite and cyst morphologies
35 seen *in vivo*.
36
37
38
39
40
41
42
43
44
45
46
47

48 **How this study might affect research, practice or policy** – Improving the accuracy
49 of identifying *Acanthamoeba* cysts and trophozoite-like structures seen on *in vivo*
50 confocal microscopy by comparing to an *ex vivo* reference standard will improve
51 diagnostic certainty, enabling the instigation of prompt anti-amoebic treatment, with
52 the potential of reducing visual loss in patients with *Acanthamoeba* keratitis.
53
54
55
56
57
58
59
60

INTRODUCTION

Acanthamoeba spp. are opportunistic pathogens of humans and can potentially cause a blinding keratitis [1]. Early stages of *Acanthamoeba* keratitis (AK) can resemble other forms of infective keratitis, which can make establishing the correct diagnosis difficult, resulting in diagnostic delay and potentially poorer visual outcome [1-3].

Current diagnostic modality for AK include culture, polymerase chain reaction (PCR) and *in vivo* confocal microscopy (IVCM). Although culture is still considered the 'gold' standard, the effectiveness of culture is suboptimal with a sensitivity rate ranging from 31 to 55% [4 5]. IVCM has been shown to be a promising tool in diagnosing AK, yielding sensitivity and specificity values of 56 to 100% and 84 to 100% [5-7]. The diagnostic criteria of AK using IVCM include the recognition of specific cystic and trophozoite-like structures with single file presentation and clustering of cystic objects to be a strong predictor of poorer visual outcome [8 9]. In validating the structures seen on IVCM, previous studies have correlated IVCM findings with *ex vivo* imaging of the organism grown on cultured plates obtained from corneal scrape or contact lens solution of the same patients [10-12] or from directly examining a suspension of cultured *Acanthamoeba* trophozoites [13]. The limitation with these approaches is that imaging findings of *Acanthamoeba* grown on a culture plate may look different to when it is in the cornea.

The aim of this study was to inoculate porcine corneas with the various forms of *Acanthamoeba* and to correlate what we see on *ex vivo* confocal microscopy (EVCM) with imaging findings from 12 culture positive AK cases on IVCM.

MATERIALS AND METHODS

Test Organism Strains and Culture

The strains used in this study were *A. castellanii* (ATCC 50370) and *A. polyphaga* (ATCC 30461). Trophozoites and cysts were produced as previously described [14 15].

Preparation of dead trophozoites and cysts

Dead *Acanthamoeba* trophozoites and cysts were prepared by exposing them to 0.02% (v/v) polyhexamethylene biguanide (PHMB) for 1 hour. After incubation the cells were visually inspected by phase contrast microscopy (x100) and cell death was confirmed by inoculating the cysts and trophozoites back into growth medium and confirming that they were non-viable. The cells were then pelleted by centrifugation at 500 x g for 5 minutes.

Preparation of empty cysts

Cysts were inoculated into Ac#6 medium for 4 hours to facilitate maximal excystation (>90%) before exposure to N-lauryl-sarcosine 0.5% (w/v) to lyse trophozoites [16]. The remaining cyst walls were pelleted by centrifugation at 1000 x g for 5 minutes and inspected microscopically to confirm >90% empty cyst.

Preparation of corneal tissue

Porcine eye globes were obtained from freshly slaughtered pigs from a local abattoir and processed as defined previously [17]. Briefly, the eye globes were immersed in sterile Povidone-iodine (0.5% w/v) for 2 minutes to facilitate decontamination before

1
2
3 neutralisation in sodium thiosulphate (0.1%, w/v). The globes were transferred to 0.1%
4
5 (w/v) gentamicin-phosphate-buffered saline (PBS) solution for 15 minutes to remove
6
7 any residual bacterial contamination before transfer to sterile saline (PBS) solution
8
9 until processing.
10
11

12 13 14 ***Acanthamoeba* inoculation**

15
16 The following *Acanthamoeba* samples were injected into different eyes sequentially:
17
18 dead trophozoites, live trophozoites, dead cyst, live cysts and empty cysts at a
19
20 concentration of 1×10^5 cells / ml. Samples were inoculated using a sterile 26-gauge
21
22 needle inserted tangentially into the middle stroma of the cornea without applying
23
24 pressure to the syringe to avoid pockets of liquid forming in the stroma. The needle
25
26 was then withdrawn slowly and the sample was inoculated into the needles path by
27
28 capillary action. Globes were imaged by EVCM immediately after inoculation with
29
30 *Acanthamoeba*.
31
32
33
34
35
36
37

38 ***Ex vivo* confocal microscopy**

39
40 EVCM was performed using the Heidelberg Retina Tomograph II with the Rostock
41
42 Corneal Module (HRT II/RCM, Heidelberg Engineering, Dossenheim, Germany). A
43
44 sterile TomoCap (Heidelberg Engineering) was mounted over the objective of the
45
46 microscope and GelTears (0.2% w/w carbomer 980, Bausch & Lomb, UK) was used
47
48 as a coupling agent between the disposable cap and the lens objective. A drop of 1%
49
50 Carmellose sodium was put on the surface of the cornea of the porcine eye inoculated
51
52 with *Acanthamoeba* and the whole eye was held secure on a standard retort stand by
53
54 a 3 prong clamp, Figure 1 Prior to inoculating the corneas with *Acanthamoeba*,
55
56 baseline IVCM images of an intact porcine cornea and a cornea after a stab incision
57
58
59
60

1
2
3 were obtained to act as a control. The instrument was then brought into contact of the
4 cornea corresponding to the area where the *Acanthamoeba* was inoculated and
5
6 multiple volume (a series of 40 images over 80µm depth) scans starting from the
7
8 superficial epithelium all the way to the deep stroma were recorded. EVCM images
9
10 were assessed qualitatively and classified based on the morphology features
11
12 detected.
13
14
15

16 17 18 19 ***In vivo* confocal microscopy**

20
21 Twelve cases, with matching morphological features to those seen on EVCM, were
22
23 selected from a cohort of cultured positive *Acanthamoeba* keratitis (AK) cases that
24
25 were published in a previous study [8]. AK staging was classified by a corneal
26
27 specialist on recruitment into the following: 1 - epitheliitis, 2 - epitheliitis with perineural
28
29 infiltrates, 3 - anterior stromal disease, 4 - deep stromal disease, and 5 - ring infiltrate.
30
31
32

33 34 35 ***Ex vivo* confocal microscopy and *in vivo* confocal microscopy image** 36 37 **comparison**

38
39 The *Acanthamoeba* morphologies identified with EVCM were used to validate the
40
41 various cyst and trophozoite-like features seen on IVCM. All available EVCM images
42
43 were reviewed by one experienced observer (SH). In total, this equated to
44
45 approximately 500 images were reviewed for each porcine cornea. Images were
46
47 reviewed anteroposteriorly from the epithelium to deep stroma. One best image
48
49 corresponding to each *Acanthamoeba* form was identified and then used as a
50
51 reference for validating structures seen on IVCM images. In addition, phase contrast
52
53 images of the various forms of *Acanthamoeba* were produced and compared with the
54
55 EVCM and IVCM images. To evaluate how cyst morphology changes with increasing
56
57
58
59
60

1
2
3 depth, a series of images obtained from a single volume stack, tracking the same
4
5 cysts, separated by 2 microns, were obtained from both EVCM and IVCM.
6
7
8
9

10 **Phase Contrast Images**

11
12 The same cell suspensions prepared for the inoculation of the corneal tissue were
13
14 used to generate the phase contrast images. Samples of each morphology were
15
16 placed onto microscope slides and overlaid with a glass coverslip. The cells were then
17
18 viewed on a Zeiss Primovert inverted microscope (Zeiss, Cambridge, UK) at a
19
20 magnification of x400 and the images were acquired on a Canon EOS M50 digital
21
22 camera using a Zeiss P95-T2 DSLR 1.6x trinocular microscope adapter.
23
24
25
26
27
28
29
30

31 **RESULTS**

32
33 The cornea of the control porcine eye showed the appearance of the intact corneal
34
35 epithelium as polygonal shaped cells with hyper-reflective cell border, with part of the
36
37 stroma containing a corneal nerve seen within its layers. The second control cornea
38
39 with a tangential incisional wound to the epithelium demonstrates an area of hypo-
40
41 reflectivity surrounded by hyper-reflectivity in the superficial and basal epithelium,
42
43 respectively (Supplementary file).
44
45
46
47
48
49
50

51 **Live *Acanthamoeba* cysts**

52
53 EVCM of live *Acanthamoeba* cysts demonstrated four main cyst morphologies: hyper-
54
55 reflective central dot with hyper-reflective outer ring, hyper-reflective central dot with
56
57 hypo-reflective outer region, stellate shaped hyper-reflective centre with hypo-
58
59 reflective outer region, and hyper-reflective round/polygonal shaped cyst (Figure 2A).
60

Representative IVCM cases with matching cyst morphologies are shown in Figure 2B-E and the patient demographics are shown in Table 1.

Patient demographics									
Case number	Age range	Sex	Duration before diagnosis	Clinical signs	Treatment	Comorbidity	Surgery	Treatment duration	Final BCVA
1	40s	F	2 weeks	D, E	PHMB	Macular off RD	PK, Phaco, RD	12 months	HM
2	10s	F	12 days	B, C	PHMB, Brolene	None	None	11 months	6/12
3	50s	F	5 weeks	D, E	PHMB	Glaucoma	PK, GDD	2 years	HM
4	20s	F	5 days	B	PHMB, Hexamidine	None	None	5 months	6/4
5	20s	F	2 weeks	B, C	PHMB, Hexamidine	None	None	8 months	6/9
6	30s	M	3 weeks	C	PHMB	None	None	13 months	6/12
7	30s	M	5 days	A	PHMB, Hexamidine	None	None	12 months	6/9
8	60s	M	4 weeks	B	PHMB, Hexamidine	None	None	9 months	6/12
9	30s	M	9 weeks	D, E	PHMB	RD, Glaucoma	PK, RD,	3 years	HM
10	20s	M	8 weeks	D, E	PHMB, Hexamidine	None	None	3 years	6/12
11	40s	F	6 weeks	C	PHMB	None	None	12 months	6/12
12	60s	F	3 weeks	A	PHMB, Hexamidine	None	None	7 months	6/6

F = female; M = male
A = epitheliitis, B = epitheliitis with perineural infiltrates, C = anterior stromal disease, D = deep stromal disease, E = ring infiltrate
GDD = glaucoma drainage device; Phaco = phacoemulsification with intraocular lens implant; RD = retinal detachment
PHMB = Polyhexamethylene biguanide; PK = penetrating keratoplasty
HM = Hand motion only

The same cyst preparation was viewed under phase contrast microscopy at x 400 and the cyst wall is seen as refractile and the double cyst wall is clearly visible (Figure 2F). The trophozoite and their cytoplasmic vacuoles show up as hyper-reflective areas inside the cyst wall that are visible on both EVCM and IVCM but they are not refractile under phase contrast. The EVCM images closely resemble those from the IVCM

1
2
3 images apart from in Case 4 (Figure 2E) where the signet ring morphology (hyper-
4 reflective outer ring with a gray/dark center) was seen on IVCM but not EVCM.
5
6 Tracking the same cysts with increasing depth revealed the cyst morphology to
7
8 change depending on which part of the cyst was imaged and this was shown in both
9
10 *ex vivo* and *in vivo* imaging (Supplementary file). In both cases, 3 types of morphology
11
12 were seen over a change in depth of 11 μm .
13
14
15
16
17
18

19 **Dead *Acanthamoeba* cysts**

20
21 Under EVCM, the main cyst morphology identified is the hyper-reflective central dot
22
23 with hypo-reflective outer region (Figure 3A) but no outer ring is seen. Hyper-reflective
24
25 round/polygonal shaped cysts are also seen but are less common and in general, the
26
27 cyst size appears much smaller compared to the live cysts. Furthermore, the hypo-
28
29 reflective outer region in dead cysts appears much darker than live cysts. Phase
30
31 contrast microscopy showed similar findings of a non-refractile outer cell wall, a
32
33 ruptured cell membrane leading to leakage of the cytoplasm, and the shrinking of the
34
35 cell with a small refractile dot inside the cyst demonstrating the remainder of the
36
37 trophozoite (Figure 3F). Representative IVCM cases, with similar cyst morphology to
38
39 the dead cysts of EVCM, are shown in Figure 3B to E (case number 5 to 8 - Table 1).
40
41 The dark hyporeflective outer rings are similar to the images from EVCM, and it is
42
43 apparent other cyst morphologies are present on IVCM, such as hyper-reflective
44
45 round/polygonal shaped cyst, amongst the dead cysts.
46
47
48
49
50
51
52
53
54

55 **Empty *Acanthamoeba* cysts**

56
57 EVCM images of empty cysts show the outerwall to be visible in some cells but they
58
59 are mainly hypo-reflective (Fig 4A). There are also small hyper-reflective dots inside
60

1
2
3 the cysts probably representing the remaining cellular material of the trophozoite.
4
5 Although this morphology was also seen in EVCM live cysts, it is much more prevalent
6
7 in empty cysts. Corresponding IVCM images from two patients (case 9 and 10), with
8
9 predominantly these features are shown in Figure 4B and C and their corresponding
10
11 clinical characteristics are shown in Table 1. Phase contrast image shows visible
12
13 mainly non-refractile cyst wall with a small amount of cellular material that has been
14
15 left behind inside the cyst by the excysting trophozoite (Figure 4D).
16
17
18
19
20
21

22 **Live trophozoites**

23
24 Under EVCM, individual cells and their cell membrane cannot be visualised, instead
25
26 trophozoites appear as a large coarse speckled area of heterogeneous hyper-
27
28 reflective material. These hyper-reflectivity dots are indicative of the food vacuoles
29
30 inside the cytoplasm of the trophozoites (Figure 5A). Representative IVCM images
31
32 from 2 cases (case 11 and 12) show similar aggregates of hyper-reflective dot like
33
34 material with no apparent discernible cell boundary seen (Figure 5B - C).
35
36
37
38

39 Similarly, the phase contrast image demonstrated live trophozoites that are amoeboid
40
41 in shape with intact non-refractile cell membrane and the cytoplasm is full of refractile
42
43 food vacuoles (Figure 5D). When the trophozoites are joined together, similar to both
44
45 EVCM and IVCM, the cell boundaries between cells are not easy to discern.
46
47
48
49
50
51
52
53
54
55
56
57
58
59
60

DISCUSSION

In this study, we have identified various forms of *Acanthamoeba* morphology using EVCM and correlated these findings with culture positive *Acanthamoeba* keratitis cases on IVCM. Various IVCM studies have been published describing the range of cyst morphologies seen in AK but there is a paucity of data corroborating IVCM findings with actual *Acanthamoeba* organism examined *ex vivo* using the same confocal microscope. The evaluation of live cysts under EVCM demonstrated four main types of cyst morphology and we found good correlation with representative culture positive cases seen on IVCM. Our EVCM findings of stellate shape hyper-reflective cysts [10], cysts with outer hyper-reflective walls [10 11], cysts with outer hypo-reflective wall, are in agreement with previous *ex vivo* and *in vivo* correlation studies.

Although all four cyst morphologies have been reported in previous IVCM studies [8 9], other phenotypes such as 'signet ring', which was detected in Case 4, and 'coffee-bean shaped' were not detected on EVCM. We found the morphology of the cyst altered depending on how the cyst was sectioned during image acquisition in terms of depth, and this might partly explain the range of cyst morphologies reported in previous IVCM studies. This assumption is further supported by the presence of a more uniform cyst morphology seen on phase contrast when the cyst images were obtained only at one particular depth.

We found dead *Acanthamoeba* cysts to be smaller, without a hyper-reflective ring, and darker hypo-reflective outer region, when compared to live cysts. This was evident

1
2
3 from the phase contrast images which showed non refractile cell wall, ruptured cell
4 membrane and shrinkage of the cysts. The comparative IVCM image showed amongst
5 the presumed dead cysts, morphologies consistent with live cysts are also present
6 within the same image. Publications on how cyst morphology change with treatment
7 are limited: Li *et al* described the cysts either disappeared or formed hollow structures
8 with anti-amoebic treatment but there was no direct *ex vivo* correlation to confirm this
9 assumption [18]. Therefore, it is difficult to ascertain whether the hollow structures
10 described were actual dead or unviable cysts or it was partly related to how the cysts
11 were sectioned on image acquisition. The morphology of the dead cysts found in this
12 study appears to be different to the hollow structures described by Li *et al* but as we
13 specifically cultured this morphology for imaging; we believe what we found is an
14 accurate description [18].
15
16
17
18
19
20
21
22
23
24
25
26
27
28
29
30
31
32

33 The main phenotype seen in empty cysts on EVCM was the central hyper-reflective
34 dot with an outer hypo-reflective wall. This appearance is likely to be related to the
35 refractile residual cellular material remaining after the trophozoite has excysted as
36 shown in the phase contrast image. Moreover, even though this phenotype was seen
37 amongst live cysts, the area surrounding the central hyper-reflective dot was much
38 darker and homogeneous compared to those seen in live cysts. There were one or
39 two cysts that had a stellate/polygonal hyper-reflective centre, similar to those seen in
40 live cysts, and this probably reflects the trophozoite failing to excyst from the cell.
41
42
43
44
45
46
47
48
49
50
51
52
53

54 In a previous *ex vivo* study using cultured samples from 8 eyes of 7 patients, Yamazaki
55 *et al* have shown trophozoites to be amorphous, highly reflective, high contrast objects
56 with no walls, and a mean size of 25.4 μm [13]. However, it is unclear how the authors
57
58
59
60

1
2
3 deduce the objects seen were in fact trophozoites by imaging a suspension of the
4 cultured medium [13]. Furthermore, they were not able to detect trophozoites in the
5 cornea, possibly because of the difficulty in distinguishing pathological features from
6 trophozoites. Shiraishi *et al* have also identified trophozoites to be highly reflective,
7 pleomorphic, organisms with presumed acanthopodia when they imaged the surface
8 of culture plate [12]. Similarly, Matumoto *et al* showed trophozoites had homogeneous
9 intense, highly reflective, multiform structures that were generally larger than 100 μm
10 in diameter on IVCM [11]. However, when they imaged the culture plate of culture
11 positive cases on light microscopy, they found the size to range between 25-50 μm ,
12 which is more in keeping with the size found by other investigators. The authors cited
13 the difference in size could be explained by the behaviour of the organisms in living
14 tissue or due to different pathogenic strains. In a previous retrospective case – control
15 study, trophozoite-like images, as defined by hyper-reflective objects with spiny
16 surface structures suggestive of acanthopodia, were one of the morphologies that was
17 found to be pathognomonic of AK [9]. In contrary to these studies, we found the
18 appearance of aggregation of trophozoites on imaging as a coarse speckled area of
19 hyper-reflective material with no distinctive separation of cell boundary seen. This was
20 confirmed by phase contrast microscopy that showed amoeboid trophozoites
21 presented with non-refractile cell membrane and multiple refractile food vacuoles
22 within the cytoplasm. Moreover, we did not identify any isolated hyper-reflective
23 objects consistent with previous definition of trophozoite-like images on EVCM [12 13].
24 We believe inoculating cultured trophozoites directly into the cornea and imaging them
25 in an *ex vivo* manner, using the same confocal microscope as *in vivo*, provides the
26 best evidence of defining the appearance of trophozoites in the cornea. The lack of
27
28
29
30
31
32
33
34
35
36
37
38
39
40
41
42
43
44
45
46
47
48
49
50
51
52
53
54
55
56
57
58
59
60

1
2
3 defined cell boundary and the way the trophozoites aggregate on the cornea explain
4 why it is difficult to identify them on imaging [19].
5
6
7
8
9

10 There are several limitations in this study. Even though the various types of cysts and
11 trophozoites were cultured using established methodology, it is possible that more
12 than one morphologies are present within each culture medium, thereby giving rise to
13 mixed morphologies on imaging. The way the organism was inoculated into the cornea
14 is not the same as how the infection is acquired *in vivo* so it is possible that cyst
15 morphologies could look different. That said, we have shown good agreement in cyst
16 morphology between EVCM and IVCM so we believe the method of inoculation would
17 not have affected the outcome. Other factors that may affect the cysts and trophozoite
18 appearance include we used cadaver porcine cornea, the corneas were imaged
19 straight after inoculation, the interaction of the host innate immune system with
20 *Acanthamoeba* may induce different morphologies to those seen *ex vivo*, and EVCM
21 images were acquired from untreated porcine corneas and then compared to IVCM
22 images from treated patients. The main strength in this study is we have imaged the
23 *Acanthamoeba* organism *ex vivo*, using the same confocal microscope, and correlated
24 the cysts and trophozoite morphologies with culture confirmed cases of AK *in vivo*.
25 This, we believe, is a robust way of confirming the various cyst and trophozoite-like
26 features seen on IVCM are indeed representative of *Acanthamoeba* in the cornea. The
27 correlation of the EVCM images taken in the absence of cytopathic effect induced by
28 drug treatment and the cells of the innate immune system with IVCM further supports
29 the reliability of the EVCM model.
30
31
32
33
34
35
36
37
38
39
40
41
42
43
44
45
46
47
48
49
50
51
52
53
54
55
56
57
58
59
60

1
2
3 In conclusion, we have described and correlated the appearance of *Acanthamoeba*
4 on EVCM with IVCM, and found good agreement in the phenotypes identified on
5 imaging. Although recent IVCM studies have found certain morphological features are
6 more sensitive in confirming a diagnosis and are indicative of a less favourable visual
7 outcome [8 9], the relationship between the prevalence of a specific cyst morphology
8 with anti-AK treatment, and how these cystic features change with time, are not known.
9
10 The changes in the prevalence of the various cyst morphologies with treatment may
11 be a useful prognostic indicator and further research is needed to elucidate the
12 relationship between cyst morphology and treatment.
13
14
15
16
17
18
19
20
21
22
23
24
25
26
27
28

29 **ACKNOWLEDGMENTS**

30
31 THE AUTHORS INDICATE NO FINANCIAL SUPPORT OR FINANCIAL CONFLICT
32 OF INTEREST. ALL AUTHORS (N.A., W.H., S.H.) were involved in all aspects of
33 article conception, writing, critical revision, and review and approval.
34
35
36
37
38
39
40
41
42
43
44
45
46
47
48
49

50 **REFERENCES**

- 51
52 1. Carnt N, Robaei D, Watson SL, Minassian DC, Dart JK. The Impact of Topical
53 Corticosteroids Used in Conjunction with Antiamoebic Therapy on the Outcome
54 of *Acanthamoeba* Keratitis. *Ophthalmology* 2016;**123**(5):984-90 doi:
55 10.1016/j.ophtha.2016.01.020[published Online First: Epub Date]].
56
57
58
59
60

- 1
2
3 2. Carnt N, Robaei D, Minassian DC, Dart JKG. Acanthamoeba keratitis in 194
4 patients: risk factors for bad outcomes and severe inflammatory complications.
5 Br J Ophthalmol 2018 doi: 10.1136/bjophthalmol-2017-310806[published
6 Online First: Epub Date]].
7
8
9
- 10 3. Robaei D, Carnt N, Minassian DC, Dart JK. The impact of topical corticosteroid use
11 before diagnosis on the outcome of Acanthamoeba keratitis. Ophthalmology
12 2014;**121**(7):1383-8 doi: 10.1016/j.ophtha.2014.01.031[published Online First:
13 Epub Date]].
14
15
16
- 17 4. Goh JWY, Harrison R, Hau S, Alexander CL, Tole DM, Avadhanam VS. Comparison
18 of In Vivo Confocal Microscopy, PCR and Culture of Corneal Scrapes in the
19 Diagnosis of Acanthamoeba Keratitis. Cornea 2018;**37**(4):480-85 doi:
20 10.1097/ICO.0000000000001497[published Online First: Epub Date]].
21
22
23
- 24 5. Tu EY, Joslin CE, Sugar J, Booton GC, Shoff ME, Fuerst PA. The relative value of
25 confocal microscopy and superficial corneal scrapings in the diagnosis of
26 Acanthamoeba keratitis. Cornea 2008;**27**(7):764-72 doi:
27 10.1097/ICO.0b013e31816f27bf[published Online First: Epub Date]].
28
29
30
- 31 6. Chidambaram JD, Prajna NV, Larke NL, et al. Prospective Study of the Diagnostic
32 Accuracy of the In Vivo Laser Scanning Confocal Microscope for Severe
33 Microbial Keratitis. Ophthalmology 2016;**123**(11):2285-93 doi:
34 10.1016/j.ophtha.2016.07.009[published Online First: Epub Date]].
35
36
37
- 38 7. Kheirkhah A, Satitpitakul V, Syed ZA, et al. Factors Influencing the Diagnostic
39 Accuracy of Laser-Scanning In Vivo Confocal Microscopy for Acanthamoeba
40 Keratitis. Cornea 2018;**37**(7):818-23 doi:
41 10.1097/ICO.0000000000001507[published Online First: Epub Date]].
42
43
44
- 45 8. Chopra R, Mulholland PJ, Hau SC. In Vivo Confocal Microscopy Morphologic
46 Features and Cyst Density in Acanthamoeba Keratitis. Am J Ophthalmol
47 2020;**217**:38-48 doi: 10.1016/j.ajo.2020.03.048[published Online First: Epub
48 Date]].
49
50
- 51 9. De Craene S, Knoeri J, Georgeon C, Kestelyn P, Borderie VM. Assessment of
52 Confocal Microscopy for the Diagnosis of Polymerase Chain Reaction-Positive
53 Acanthamoeba Keratitis: A Case-Control Study. Ophthalmology
54 2018;**125**(2):161-68 doi: 10.1016/j.ophtha.2017.08.037[published Online First:
55 Epub Date]].
56
57
58
59
60

- 1
2
3
4
5
6
7
8
9
10. Kobayashi A, Ishibashi Y, Oikawa Y, Yokogawa H, Sugiyama K. In vivo and ex vivo laser confocal microscopy findings in patients with early-stage acanthamoeba keratitis. *Cornea* 2008;**27**(4):439-45 doi: 10.1097/ICO.0b013e318163cc77[published Online First: Epub Date]].
11. Matsumoto Y, Dogru M, Sato EA, et al. The application of in vivo confocal scanning laser microscopy in the management of Acanthamoeba keratitis. *Mol Vis* 2007;**13**:1319-26
12. Shiraishi A, Uno T, Oka N, Hara Y, Yamaguchi M, Ohashi Y. In vivo and in vitro laser confocal microscopy to diagnose acanthamoeba keratitis. *Cornea* 2010;**29**(8):861-5 doi: 10.1097/ICO.0b013e3181ca36b6[published Online First: Epub Date]].
13. Yamazaki N, Kobayashi A, Yokogawa H, et al. Ex vivo laser confocal microscopy findings of cultured Acanthamoeba trophozoites. *Clin Ophthalmol* 2012;**6**:1365-8 doi: 10.2147/OPHTH.S35258[published Online First: Epub Date]].
14. Heaselgrave W, Hamad A, Coles S, Hau S. In Vitro Evaluation of the Inhibitory Effect of Topical Ophthalmic Agents on Acanthamoeba Viability. *Transl Vis Sci Technol* 2019;**8**(5):17 doi: 10.1167/tvst.8.5.17[published Online First: Epub Date]].
15. Hughes R, Heaselgrave W, Kilvington S. Acanthamoeba polyphaga strain age and method of cyst production influence the observed efficacy of therapeutic agents and contact lens disinfectants. *Antimicrobial agents and chemotherapy* 2003;**47**(10):3080-4
16. Kilvington S, Heaselgrave W, Lally JM, Ambrus K, Powell H. Encystment of Acanthamoeba during incubation in multipurpose contact lens disinfectant solutions and experimental formulations. *Eye Contact Lens* 2008;**34**(3):133-9 doi: 10.1097/ICL.0b013e3181772c95
00140068-200805000-00001 [pii][published Online First: Epub Date]].
17. Parekh M, Ferrari S, Di Iorio E, et al. A simplified technique for in situ excision of cornea and evisceration of retinal tissue from human ocular globe. *J Vis Exp* 2012(64):e3765 doi: 10.3791/3765[published Online First: Epub Date]].
18. Li S, Bian J, Wang Y, Wang S, Wang X, Shi W. Clinical features and serial changes of Acanthamoeba keratitis: an in vivo confocal microscopy study. *Eye (Lond)*

1
2
3 2020;**34**(2):327-34 doi: 10.1038/s41433-019-0482-3[published Online First:
4 Epub Date]].

- 5
6
7 19. Hau SC, Dart JK, Vesaluoma M, et al. Diagnostic accuracy of microbial keratitis
8 with in vivo scanning laser confocal microscopy. Br J Ophthalmol
9 2010;**94**(8):982-7 doi: 10.1136/bjo.2009.175083[published Online First: Epub
10 Date]].
11
12
13
14
15
16
17
18
19
20
21
22
23
24
25
26
27
28
29
30
31
32
33
34
35
36
37
38
39
40
41
42
43
44
45
46
47
48
49
50
51
52
53
54
55
56
57
58
59
60

Confidential: For Review Only

FIGURE LEGENDS

Figure 1.

Ex vivo scanning process. *Ex vivo* confocal microscopy imaging of the cornea of the porcine eye globe with the Heidelberg Retina Tomograph II/Rostock Corneal Module laser confocal microscope. The image shows the eye globe held in place using a three-pronged clamp attached to a retort stand with the cornea in contact with the TomoCap during the scanning process.

Figure 2.

Morphological classification of live cysts observed with *ex vivo* confocal microscopy, *in vivo* confocal microscopy and phase contrast imaging. (A) *Ex vivo* confocal microscopy. (B) *In vivo* confocal microscopy of Case 1. (C) *In vivo* confocal microscopy of Case 2. (D) *In vivo* confocal microscopy of Case 3. (E) *In vivo* confocal microscopy of Case 4. (F) Phase contrast images. Labels: hyper-reflective central dot with hyper-reflective outer ring (star), hyper-reflective central dot with hypo-reflective outer region (arrow head), stellate shaped hyper-reflective centre with hypo-reflective outer region, (arrow), hyper-reflective round/polygonal shaped cyst (dotted arrow), signet ring (cross).

Figure 3.

Morphological classification of dead cysts observed with *ex vivo* confocal microscopy, *in vivo* confocal microscopy and phase contrast imaging. (A) *Ex vivo* confocal microscopy. (B) *In vivo* confocal microscopy of Case 5. (C) *In vivo* confocal microscopy of Case 6. (D) *In vivo* confocal microscopy of Case 7. (E) *In vivo*

1
2
3 confocal microscopy of Case 8. (F) Phase contrast image. Labels: hyper-reflective
4 central dot with hyper-reflective outer ring (star), hyper-reflective central dot with
5 hypo-reflective outer region (arrow), hyper-reflective round/polygonal shaped cyst
6 (dotted arrow)
7
8
9
10
11
12
13
14

15 **Figure 4.**

16 Morphological classification of empty cysts observed with *ex vivo* confocal
17 microscopy, *in vivo* confocal microscopy and phase contrast imaging. (A) *Ex vivo*
18 confocal microscopy. (B) *In vivo* confocal microscopy of Case 9. (C) *In vivo* confocal
19 confocal microscopy of Case 10. (D) Phase contrast image. Labels: hyper-reflective central
20 dot with hypo-reflective outer region (arrow head), hyper-reflective round/polygonal
21 shaped cyst (dotted arrow), stellate shaped hyper-reflective centre with hypo-
22 reflective outer region (arrow).
23
24
25
26
27
28
29
30
31
32
33
34
35

36 **Figure 5.**

37 Appearance of trophozoites on *ex vivo* confocal microscopy, *in vivo* confocal
38 microscopy and phase contrast imaging. (A) *Ex vivo* confocal microscopy indicating
39 an irregular area of heterogeneous hyper-reflectivity (boundary demarcated by
40 arrows). (B) *In vivo* confocal microscopy of Case 11 showing an area of
41 heterogeneous hyper-reflectivity that is similar to 4A (arrows). (C) *In vivo* confocal
42 confocal microscopy of Case 12 showing 2 areas of heterogeneous hyper-reflectivity (arrows)
43 and hyper-reflective round/polygonal shaped cysts (dotted arrow). (D) Phase
44 contrast image showing multiple trophozoites and their food vacuoles, with some
45 cells possessing acanthopodia.
46
47
48
49
50
51
52
53
54
55
56
57
58
59
60



Figure 1

196x196mm (93 x 93 DPI)

1
2
3
4
5
6
7
8
9
10
11
12
13
14
15
16
17
18
19
20
21
22
23
24
25
26
27
28
29
30
31
32
33
34
35
36
37
38
39
40
41
42
43
44
45
46
47
48
49
50
51
52
53
54
55
56
57
58
59
60

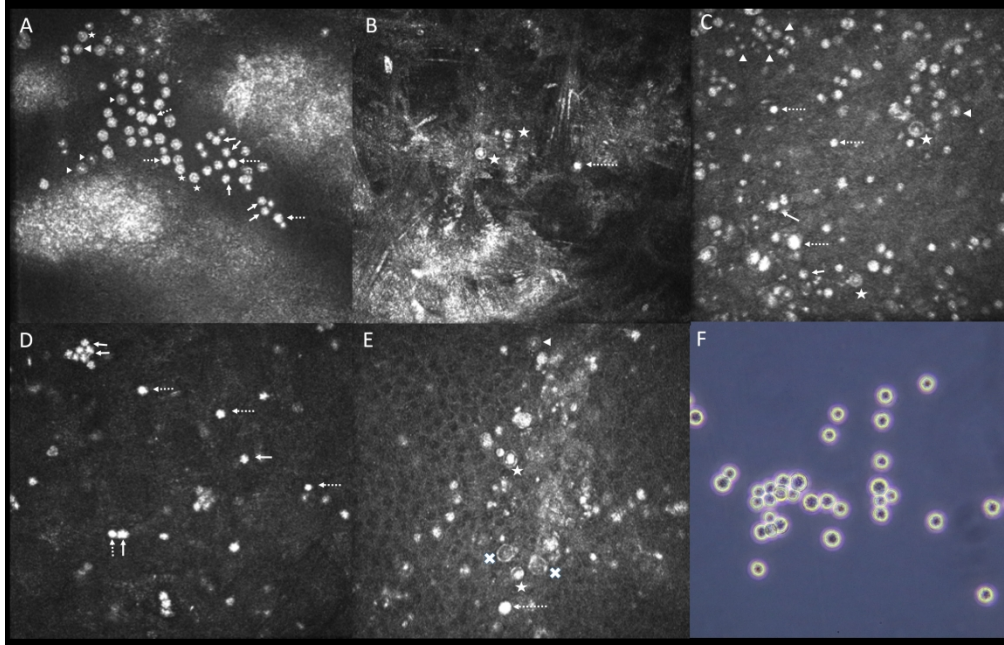


Figure 2

547x352mm (150 x 150 DPI)

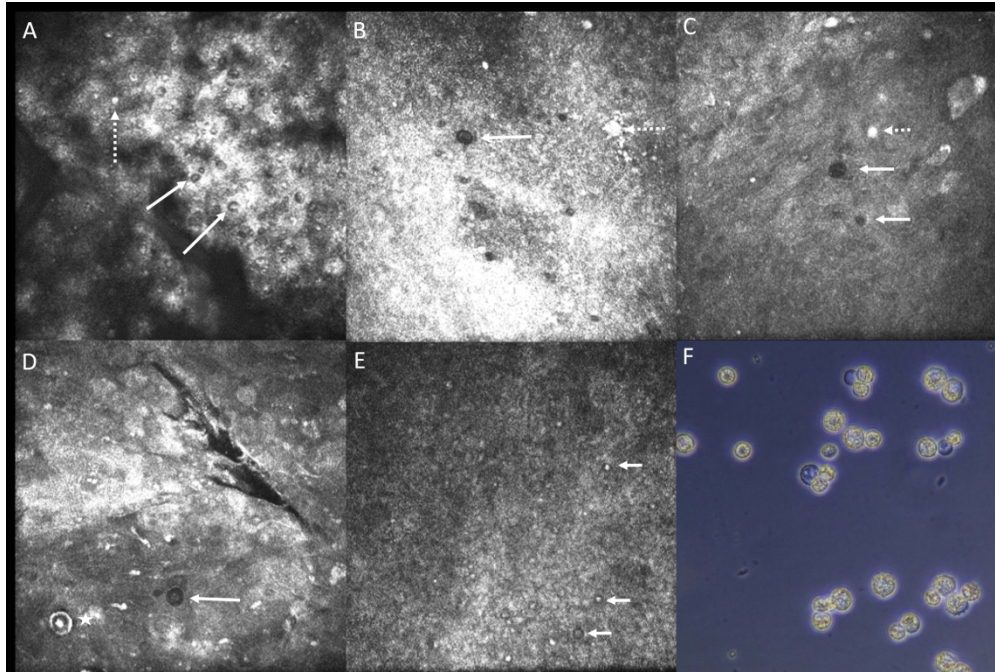


Figure 3

495x332mm (150 x 150 DPI)

1
2
3
4
5
6
7
8
9
10
11
12
13
14
15
16
17
18
19
20
21
22
23
24
25
26
27
28
29
30
31
32
33
34
35
36
37
38
39
40
41
42
43
44
45
46
47
48
49
50
51
52
53
54
55
56
57
58
59
60

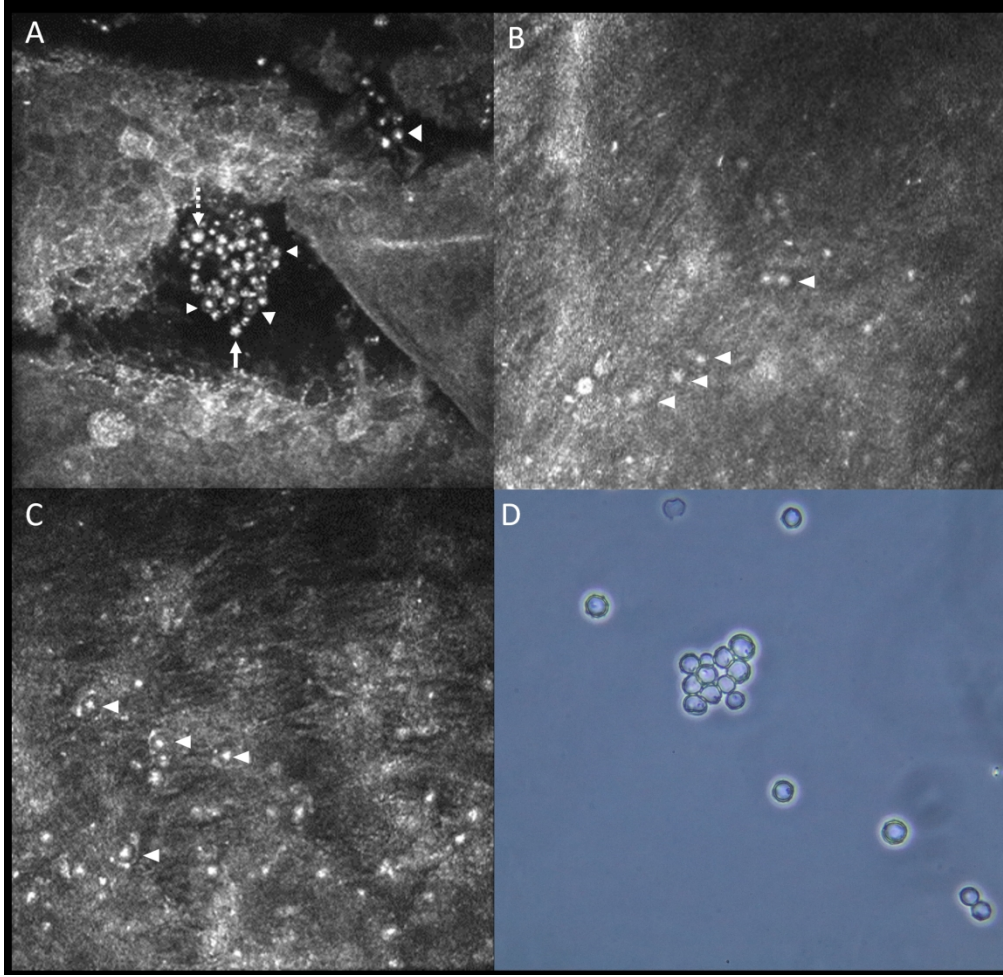


Figure 4

371x361mm (150 x 150 DPI)

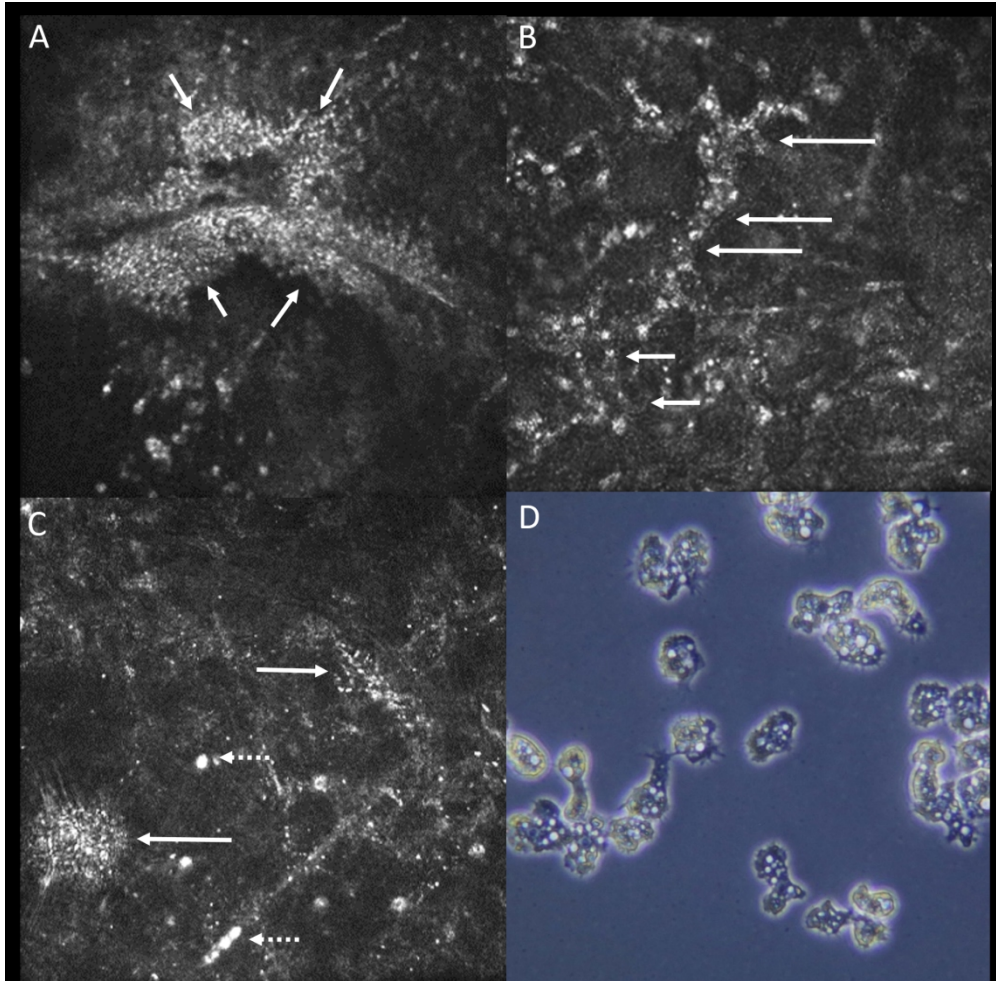


Figure 5

347x340mm (150 x 150 DPI)

SUPPLEMENTAL FIGURE LEGENDS

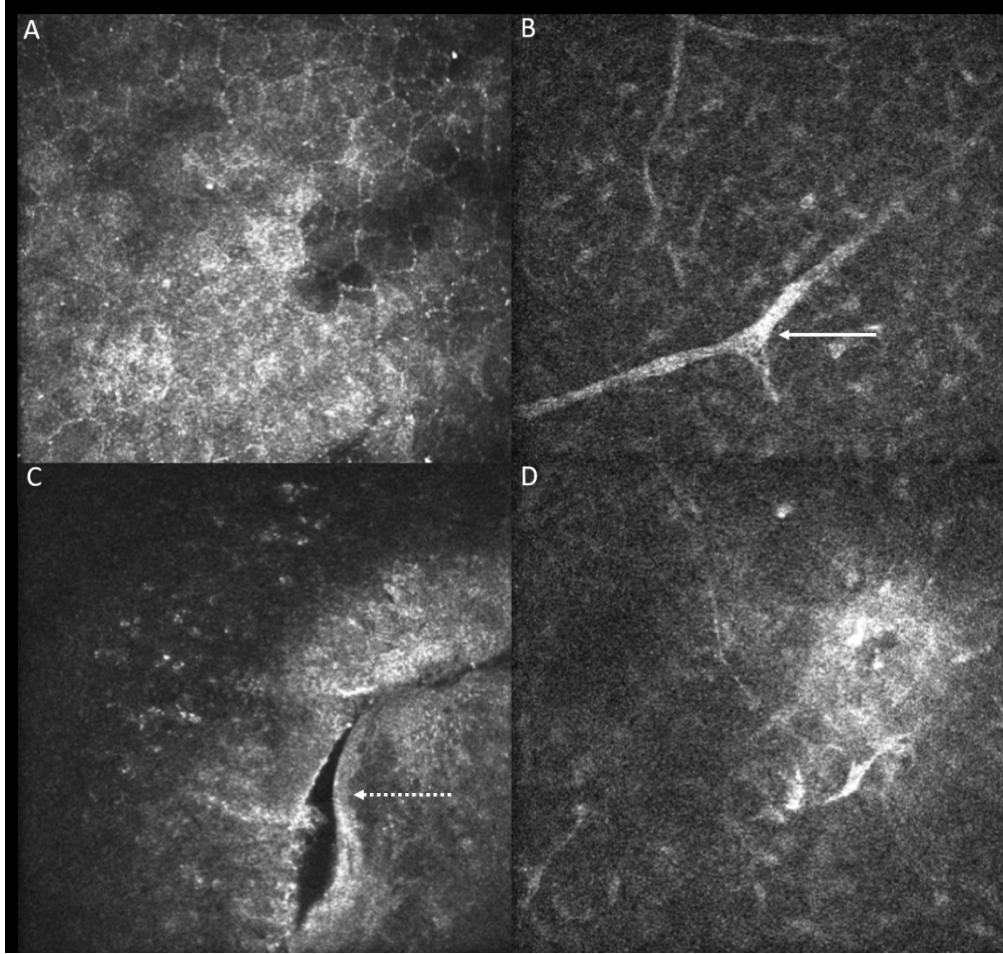
Supplemental Figure 1.

Ex vivo microscopy images of porcine cornea. (A) Corneal epithelium. (B) Anterior stroma showing the presence of a corneal nerve (arrow); depth = 70 μm . (C) Tangential incisional wound penetrating the epithelium (dotted arrow). (D) Area of hyper-reflectivity in the basal epithelium beneath the incisional wound of image 2C; depth = 55 μm .

Supplemental Figure 2.

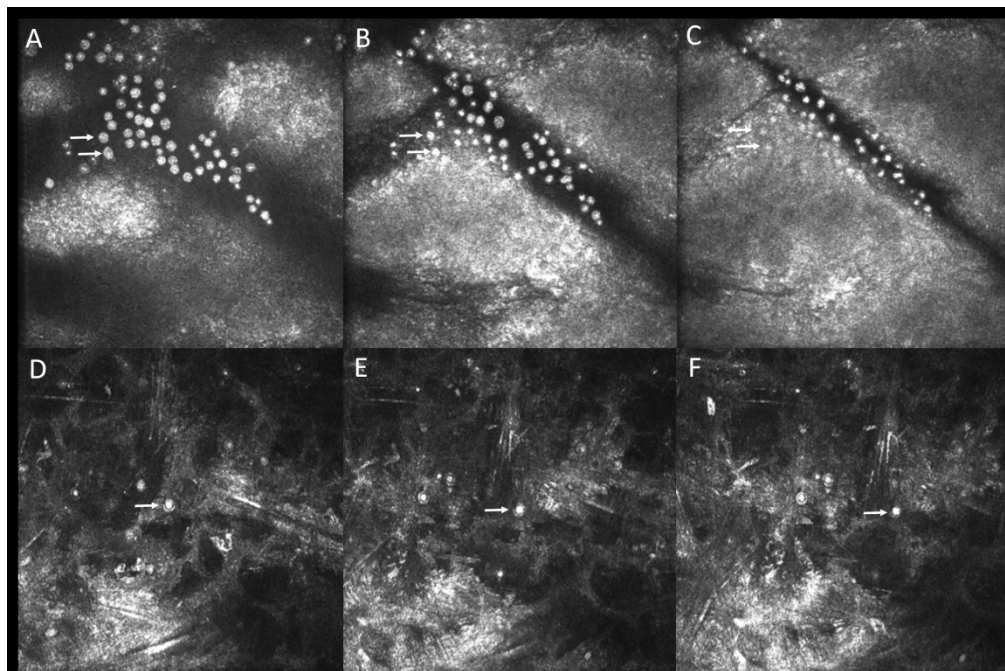
Alteration in cyst morphology with increasing depth. (A-C) *Ex vivo* confocal microscopy of live cysts: (A) Hyper-reflective central dot with hyper-reflective outer ring, depth = 13 μm ; (B) hyper-reflective round/polygonal shaped cyst, depth = 20 μm ; (C) hyper-reflective central dot with hypo-reflective outer region, depth = 24 μm . (D-F) *In vivo* confocal microscopy of a case cultured positive for *Acanthamoeba*: (D) Hyper-reflective central dot with hyper-reflective outer ring, depth = 122 μm ; (E) hyper-reflective central dot with hypo-reflective outer region, depth = 129 μm ; (F) hyper-reflective round/polygonal shaped cyst, depth = 133 μm .

1
2
3
4
5
6
7
8
9
10
11
12
13
14
15
16
17
18
19
20
21
22
23
24
25
26
27
28
29
30
31
32
33
34
35
36
37
38
39
40
41
42
43
44
45
46
47
48
49
50
51
52
53
54
55
56
57
58
59
60



287x274mm (150 x 150 DPI)

1
2
3
4
5
6
7
8
9
10
11
12
13
14
15
16
17
18
19
20
21
22
23
24
25
26
27
28
29
30
31
32
33
34
35
36
37
38
39
40
41
42
43
44
45
46
47
48
49
50
51
52
53
54
55
56
57
58
59
60



426x283mm (150 x 150 DPI)